IAC-04-IAA-3.8.2.10

ON THE PERFORMANCE OF A MOTORIZED TETHER USING A BALLISTIC LAUNCH METHOD

David J. McKenzie

PhD Student,
Department of Mechanical Engineering, University of Glasgow, G12 8QQ, Scotland, UK
d.mckenzie@mech.gla.ac.uk

Matthew P. Cartmell

Professor of Applied Dynamics,
Department of Mechanical Engineering, University of Glasgow, G12 8QQ, Scotland, UK
m.cartmell@mech.gla.ac.uk

Abstract: In order to launch mankind into deep space a staging base must be built on the moon, or in space, to gain experience of the extra-terrestrial environment and to test the critical technologies needed. In view of this, this paper outlines a low-cost, reusable method for payload transfer to the moon using a Motorized Momentum Exchange Tether. The performance of the Motorized Momentum Exchange Tether (MMET) is predicted by simulation of the equations of motion of a pair of identical propulsion tethers emanating from the rotor of a central motorized facility with two identical payloads, one at the end of each tether. Suitable reaction is provided by a pair of similarly structured counter-rotating stabilizing stators comprising tethers attached to the central facility, conventionally known as the outrigger system. The outer payload gains the required ΔV by means of the motor torque which angularly accelerates both the payloads with respect to a reference frame fixed at the centre of rotation, and then converts the resultant angular momentum to linear momentum by releasing both payloads from the propulsion tethers. Thus, the absolute velocity of the outer payload is the orbital velocity plus this increment due to motorized spin-up. The inner payload's absolute velocity is the orbital velocity minus the increment due to motorized spin-up. Momentum is, of course, conserved across the system. A demonstration mission to transfer a payload from LEO to Lunar Capture is proposed in this paper. It uses the Weak Stability Boundary (WSB) method, successfully demonstrated by the Hiten mission, to launch ballistically to Lunar Capture Orbit with a relatively minor $50ms^{-1}$ capture burn. This method is particularly suited to launching with tethers, because the small capture burn replaces the large circularization burn traditionally used with Hohmann transfers. The propulsion time will be acceptable for most payloads; 100 days using ballistic transfer compared to 4 days with chemical propulsion and 500 days for the ESA SMART1 mission using ion propulsion. It is important to note that transfers based on motorized tethers would be unsuitable for live organic payloads given the relatively high centripetal accelerations involved in the spin-up.

Keywords: Orbital Tether, Ballistic Launch, Momentum Exchange Tether, MMET, Weak Stability Boundary, WSB, Tether

Background

Orbital Tethers are well known to have great potential for an important role in the space industry. The underlying theme of all space launches has always been to get a payload to its destination safely, accurately, economically, and reliably. However, shrinking budgets demand that this be achieved for lower mass and at lower cost than ever before. With Motorized Momentum Exchange Tethers (MMETs) it may be possible to achieve these goals for a lower mass and a lower ΔV certainly when compared with chemical propulsion, and potentially with other forms of propulsion too.

History

The idea of a tether in the form of a long line which can be used in an ingenious way to move mass is not new, indeed Tsiolkovsky's space elevator concept was first proposed in 1895. Since then there have been many different proposals for exploiting momentum transfer using this sort of system; see [1] for more details. The extension of the general tether concept into a symmetrical motorized system with two payloads, in the form of Cartmell's MMET concept, was made relatively recently in 1996 and first published in 1998 [2]. Further work by Ziegler and Cartmell led to an overview of hanging, spinning, and motorized tethers considered as 2D planar systems in equatorial Earth orbit [3]. Research by Ziegler [4] into the planar and three dimensional dynamics of various rigid-body conceptualizations in certain orbital configurations has shown that a vast range of different motions and phenomena are potentially possible. Conditions have also been identified for a practically useful performance [4]. This paper extends the equations of a dumb-bell tether system to a generalized inclined orbit incorporating planar and non-planar motions of the tethers [5]. The model accounts for payload and facility mass and includes a simple model of the tether mass. A more advanced tether mass model will be incorporated in the next level of modelling. The Weak Stability Boundary (WSB) method was proposed by Belbruno [6] in 1987 and has been developed by Belbruno and Miller [7] and Koon et al [8]. The WSB method relies on Earth-Sun-Moon gravitational interaction in the region where chaotic dynamics occur to capture a payload launched from the Earth with a reduced ΔV cost.

Rationale

The WSB transfer is ideally suited to tether launched payloads. To show this, a comparison between the Hohmann transfer with chemical rockets and the WSB method can be made. In the Hohmann method, the payload rocket fires once to transfer from LEO to Lunar Transfer Orbit, and once again to capture to Lunar Orbit. In the WSB method, the payload is transferred on a ballistic trajectory tangentially away from the Earth with the vast majority of the ΔV imparted in LEO, with a minimal capture burn of around $20 - 50\ ms^{-1}$ to capture around the moon. There are significant savings in the three main areas of concern for engineers. The ΔV cost may be reduced by around $100 - 200\ ms^{-1}$; the mass budget may be reduced by installing a smaller engine, or by only using manoeuvring thrusters for the capture; and the volume may be saved by carrying less propellant in smaller fuel tanks to the moon. Moreover, the MMET system is reusable, and the payloads would, in all practical deployments, be transported to orbit separately from the central facility, which would be taken up once and then subject merely to routine servicing and necessary orbital maintenance manoeuvres.

Equations

To bring the MMET concept closer to deployable reality, a further programme of simulations of different system models is required. The following analysis has been programmed into Mathematica^{TM} and the resultant equations of motion have been solved numerically within the program, according to the requirements of the Lunar Transfer mission. The modelling paradigm assumes a rigid body dumb-bell tether, complete with the massive, centrally located, motorized facility, and assigns generalized co-ordinates for planar spin, non-planar pitch, instantaneous orbital inclination [5], orbit radius, and true anomaly. The analysis is summarized next, starting with the appropriate transformation matrices for rotation.

Rotations

Three Vector Rotation matrices are set up to describe the direction of a single 3D vector about its origin using the Aerospace sequence of Euler angle rotations. The payloads, stator / outrigger sub-system, hub, and the tethers are all idealised as point masses. The location of each is found by rotating the mass point by means of three rotation matrices, in the order $R_{\beta,X}.R_{\alpha,Y}.R_{\psi,Z}$ about the tether system common centre of mass (COM) so the vector of each mass is aligned with the Earth Gravity Vector, $\vec{X}_0$. The position vector of the Payload masses before the rotation about the tether COM are shown in Figure 1.1, after the α rotation about the tether COM in Figure 1.2 and after the rotation of ψ about the tether COM in Figure 1.3.

$$R_{\beta,X} = \begin{bmatrix} 1 & 0 & 0 \\ 0 & \cos[\beta] & -\sin[\beta] \\ 0 & \sin[\beta] & \cos[\beta] \end{bmatrix} \quad (1)$$

$$R_{\alpha,Y} = \begin{bmatrix} \cos[\alpha] & 0 & \sin[\alpha] \\ 0 & 1 & 0 \\ -\sin[\alpha] & 0 & \cos[\alpha] \end{bmatrix} \quad (2)$$

$$R_{\psi,Z} = \begin{bmatrix} \cos[\psi] & -\sin[\psi] & 0 \\ \sin[\psi] & \cos[\psi] & 0 \\ 0 & 0 & 1 \end{bmatrix} \quad (3)$$

Once the rotations have been performed on the system about the tether COM, the radius vector from the centre of the Earth to the centre of mass of the tether body system is added to give the position of the masses in Earth Inertial space. The position vectors of the masses in Earth inertial space are then rotated about the centre of the Earth by the rotation matrices $R_{\gamma,X}.R_{i,Y}.R_{\theta,Z}$ to align the tether X-axis with the first point of Aries. The position vector of the Payload masses before the rotation about the centre of the Earth are shown in Figure 1.3, after the i rotation about the centre of the Earth in Figure 1.4 and after the rotation of θ about the centre of the Earth in Figure 1.5.

The Payload Position vector is shown in Equation 4:

$$P_{Payload} = \begin{bmatrix} \cos[i+\alpha]\cos[\theta+\psi]L_{tether} \\ \cos[i+\alpha]\sin[\theta+\psi]L_{tether} \\ -\sin[i+\alpha]L_{tether} \end{bmatrix} \quad (4)$$

The β and γ rotations are set to zero because previous work has suggested that the roll is likely to be considerably smaller than either the pitch (α) or the yaw (ψ), and so for the time being this condition will be maintained. The negative sign of the z component is a consequence of the z axis pointing from the centre of the Earth through the South Pole as implicitly specified in the Aerospace rotations sequence.

The first derivative of the positions of the masses with respect to time are taken to give the velocities of the masses. These derivative vectors, combined with the position vectors, are used to give expressions for:

1. Translational Kinetic Energy $\frac{1}{2}m_jV_j^2$
2. Rotational Kinetic Energy $\frac{1}{2}I_j\omega_j^2$
3. Gravitational Potential Energy $-\frac{\mu m_j}{R_j}$

These expressions for the energy of the system are used to find the Lagrangian of the system. The governing equations for the system are found using $\frac{d}{dt}[\frac{\partial T}{\partial \dot{q}_j}] - \frac{\partial T}{\partial q_j} = Q_j$ where q_j is replaced by the chosen generalized co-ordinates, $i, \psi, \alpha, R, \theta$, to give five non-linear and coupled equations in the five unknown variables: instantaneous inclination, in-plane tether angle, out-of-plane tether angle, radius of the COM and the true anomaly of the COM. The inclination variable is referred to as instantaneous to distinguish it from the constant orbit parameter of orbital inclination. This is analogous to the difference between the variable true anomaly and the constant right ascension of the ascending node.

The non-conservative force is represented by Q_j and can be evaluated by considering the virtual work done by the motor torque summed over each mass:

$$Q_j = \sum_{mass} F.\frac{\partial P_{mass}}{\partial j} \quad (5)$$

with j as the chosen generalized co-ordinates $i, \psi, \alpha, R, \theta$ and P_{mass} as the position vector of the mass under consideration.

The 3x3 rotation matrix for a generalized rotation in the tether body axes, excluding roll, as given previously is multiplied by the length vector to give the position of each mass in the tether body axes :

$$P_{mass} = R_{\alpha,Y_B}.R_{\psi,Z_B}.\begin{pmatrix} L_{mass} \\ 0 \\ 0 \end{pmatrix} \quad (6)$$

The resultant 3x1 vector is differentiated with respect to each of the five chosen generalized co-ordinates, $i, \psi, \alpha, R, \theta$, to give a 5x3 matrix. The force vector expressed in tether body axes is then found by multiplying the generalized rotation matrix by the force vector:

$$Force = R_{\gamma,X_B}.R_{\alpha,Y_B}.R_{\psi,Z_B}.\begin{pmatrix} 0 \\ \tau/L_{mass} \\ 0 \end{pmatrix} \quad (7)$$

The dot product of the 3x1 force vector and the 5x3 matrix then gives a 5x1 vector containing the Q_j terms for the chosen generalized co-ordinates $i, \psi, \alpha, R, \theta$ to be used in the right hand side of the equations of motion.

Spacecraft Sizing

The MMET system is sized to launch a 10 kg payload to Lunar capture orbit. This is intended as a demonstration level mission, although the MMET system may be scaled to launch larger payloads, as discussed previously [1, 2, 3, 4, 5].

The facility is entirely housed within a cylinder containing the motor and gearbox. The solar arrays will consist of 35000 standard sized 2 cm x 4 cm solar cells, which provide the power required by the motor, recharge the batteries and provide power to the spacecraft bus. The solar cells will be a *InGaP/GaAs/Ge* type capable of 25% efficiency [9], with a degradation rate of 1*%/year* [10]. The mission length of 5 years is based on the probability of a tether cut due to orbital debris when using multiple redundant tether strands, coupled with the useful life of the solar arrays.

The power to the motor will only be available during the time the facility is not in eclipse and this is factored into the equations using the function "Eclipse" shown in Appendix 2. This function tests to see if the facility is in Earth's shadow; if the facility is in shadow, the right hand side of the governing equations are multiplied by zero thereby stopping the motor from accelerating the rotor.

The total useful power available for a 2 m x 3 m cylinder augmented by a 1.5 m x 6 m fold out panel will be 4.3 kW when launched and 3.05 kW at the end of a 5 year mission. The end of life power allows the motor characteristics to be defined, in this case the motor used will be a 3 kW rated motor capable of driving 1000 Nm of torque through a reducing gearbox. The gearbox will reduce the rotations from the motor armature rotation of 430 $rads^{-1}$ to the required angular velocity of the rotor arm of 20 $rads^{-1}$. This motor is based around GE Industrial DC motor model 5BC49JB1115, rated at 4hp and 4150 RPM, which is designed to drive an electric vehicle.

The rotor is comprised of two 1km tether sections with each linking the facility to the payloads. The stator is identical, with the payloads replaced by counterweights. The tether itself is Zylon^{TM} fibre with a tensile strength of 5.8 GPa, density of 1570 kgm^{-3} and cross sectional area of 64 mm^2. This leads to a tether mass of 100 kg for each of the four tether lines, totalling 400 kg. A safety factor of 1.3 is applied to the calculation of breaking stress, however additional precautions must be taken by careful design of the tether structure to ensure the tether will remain intact if impacted by micro-meteorites or debris [11].

The tether mass outweighs the payload mass in order to keep the breaking stress to a manageable level. This is advantageous as the tethers may be adjusted to compensate for any tether failure mode or asymmetric payload release.

The MMET is designed to be highly reusable. The 5 day spin up cycle must be matched by an equal 5 day spin down cycle to return the rotor to a stationary position aligned with the gravity vector. When this is achieved, the payload will be much easier to dock than when in motion. For the WSB transfer, payloads can be transferred to the Moon every lunar month, leaving a window of 20 days to dock the payloads to the tethers.

Analysis

The square of the characteristic velocity, U, of the tether is proportional to the tensile strength, T, and inversely proportional to the density, ρ:

$$U = \sqrt{\frac{2T}{\rho}} \tag{8}$$

The characteristic velocity determines the maximum velocity attainable for a tether supporting its own mass while rotating. Adding a payload limits the velocity a tether can impart by increasing the tension and stress in the tether, therefore by keeping the mass of the payload to a fraction of the tether's mass, the decrease in characteristic velocity is minimised. A tether manufactured from Zylon™ with $T = 5.9\ GPa$, $\rho = 1570\ kgm^{-3}$ with a safety factor of 1.3 gives a characteristic velocity of $2.238\ kms^{-1}$. With a payload mass equivalent to 10% of the tether mass attatched to the end of the tether, the characteristic velocity will drop by approximately 10% to $2.10\ kms^{-1}$. To achieve Lunar orbit, the payload will need $3.187\ kms^{-1}$ [12] from LEO at 167 km altitude. Therefore, the tether will have to occupy a higher earth orbit of 1000 km to successfully launch to the moon, or a staged system will be required [5].

Simulation Assumptions

The equations of motion were simulated in Mathematica™ using the internal numerical solution routine NDSolve. Several simplifying assumptions were made so the simulation will execute in a reasonable length of time on a computer.

The rigid body assumption represents the tether as a dumb-bell within which there is no flexure and so the excitation provided by the facility against the outrigger sub-system manifests solely as rigid body rotation of both the propulsion and the outrigger sub-systems, noting that only the propulsion side is treated in this paper. Therefore phenomena such as phase-lag and local vibrations are not modelled, although there is no doubt that they would occur to some extent in a real physical system. It is, however, quite reasonable to assume rigid body behaviour of a tether in space once it is rotating at its design speed, particularly as any practical implementation would use torque or reeling control to remove unwanted vibrations [13].

The tether mass is idealized to a point mass at the midpoint of the tether. This will cause the gravitational potential energy of the tether to be slightly inaccurate and will warrant correction in subsequent models. Ziegler has proposed a solution [4] to idealize the tether as a series of discrete masses along the length of the tether to approximate the continuous mass distribution of the tether; for 20 discretizations, the tether is accurately modelled.

The stator arm has not been modelled. This will mean that the rotor-stator interactions are not present and will warrant further investigation.

Simulation Results

The simulation was executed for a time of $432000s$ with the initial conditions: $i'[0] = \psi'[0] = \alpha'[0] = R'[0] = \theta'[0] = 0$, $i[0] = 29^\circ$, $\psi[0] = \alpha[0] = 0^\circ$, $R[0] = 7378\ km$, $\theta[0] = 0$, $orbital\ eccentricity = 0$, $\tau = 1000\ Nm$, $M_{payload} = 10\ kg$, $M_{tether} = 100\ kg$, $M_{facility} = 500\ kg$ and $L_{tether} = 1\ km$.

As is seen in Figure 2.6, the in-plane angle ψ is accelerated from its initial condition when in sunlight. The out of plane angle α in Figure 2.3 oscillates in synchronisation with the instantaneous orbital inclination, i, in Figure 2.1. This is shown in more detail in Figures 2.2 and 2.4. The out of plane angle will make directing the tether payload difficult as the required release direction will not be constantly in the tether plane. Careful timing and control of the release must be achieved to send the payload to reach the Moon via the WSB trajectory.

The ΔV reaches the $2.10\ kms^{-1}$ required to use the WSB transfer trajectory, as shown in Figure 2.5, just before the stress in the tether reaches the maximum safe working stress. The ΔV graph is a stepped line due to the Eclipse function; the MMET is only accelerating the payloads when the facility is in sunlight.

Weak Stability Boundary

The Weak Stability Boundary (WSB) method has been described in the literature [6, 7, 8]. To summarise, the WSB utilises the Earth-Sun-Moon interaction to lower the ΔV required to capture a satellite in lunar orbit. The WSB can be thought of as two Circular Restricted Three Body Problems (CR3BP) patched together with a small correction burn of less than $25ms^{-1}$ at the boundary between the Sun-Earth system and the Earth-Moon system.

A patch point is located by integrating forward the dynamics of the spacecraft in the Earth-Moon system from the patch point until the spacecraft is ballistically captured in Lunar Orbit, and simultaneously integrating backward the dynamics of the spacecraft in the Sun-Earth system until the spacecraft links up with a LEO orbit around the Earth. Thus a patch point is found along with two halves of the trajectory from LEO to ballistic capture in Lunar orbit via the patch point.

Once the spacecraft is ballistically captured around the moon, a small thrust is required to ensure that the spacecraft does not have the energy to escape. A ΔV of less than $50ms^{-1}$ will fix the spacecraft in a highly elliptical ($e = 0.9$) but stable Lunar orbit.

A midpoint burn of $\Delta V = 25\,ms^{-1}$ with a capture burn of $\Delta V = 50ms^{-1}$ corresponds to a fuel mass fraction of 9.6% assuming an I_{sp} rating of $75s$ for a Nitrogen cold gas thruster. A conservative estimate of 1 kg mass for the engine and associated structure leaves the 10 kg original satellite mass with 8.04 kg of useful payload mass.

Conclusions

The Weak Stability Boundary method is particularly suited to use with a Motorized Momentum Exchange Tether. It has been demonstrated that a micro-satellite payload can be launched by this method at a rate of once per month throughout the life of the mission. The MMET may be used to deliver multiple micro-satellites containing a science payload to lunar orbit, or the design can be scaled up to provide supplies to a lunar base.

Acknowledgements

The research of DJM is supported by an EPSRC Postgraduate Research Studentship, which is gratefully acknowledged.

References

[1] M. Eiden and M.P. Cartmell. Overcoming the challenges: Tether systems roadmap for space transportation applications. *AIAA/ICAS International Air and Space Symposium and Exposition, Dayton, Ohio, USA.*, 14-17 July 2003.

[2] M.P. Cartmell. Generating velocity increments by means of a spinning motorised tether. *34th AIAA/ASME/SAE/ASEE Joint Propulsion Conference and Exhibit, Dayton, Ohio, USA*, 98-3739, 13-15 July 1998.

[3] S.W. Ziegler and M.P. Cartmell. Using motorized tethers for payload orbital transfer. *Journal of Spacecraft and Rockets*, 38(6):904–913, 2001.

[4] S.W. Ziegler. *The Rigid Body Dynamics of Tethers in Space*. PhD thesis, Department of Mechanical Engineering, University of Glasgow, 2003.

[5] M.P. Cartmell, C.R. McInnes, and D.J. McKenzie. Proposals for an earth-moon mission design based on motorised momentum exchange tethers. *Advanced Problems in Mechanics APM2004, Russian Academy of Sciences, St.Petersburg*, June 24 - July 1 2004.

[6] E.A. Belbruno. Lunar capture orbits, a method of constructing earth moon trajectories and the lunar GAS mission. *DGLR, and JSASS, International Electric Propulsion Conference,19th, Colorado Springs, CO, USA*, AIAA-1987(1054):1–10, 1987.

[7] J.K. Miller and E.A. Belbruno. A method for the construction of a lunar transfer trajectory using ballistic capture. *Spaceflight Mechanics: Advances in the Astronautical Sciences, AAS 91-100*, 75(1):97–109, 1991.

[8] W.S. Koon, M.W. Lo, J.E. Marsden, and S.D. Ross. Low energy transfer to the moon. *Celestial Mechanics and Dynamical Astronomy*, 81(1-2):63–73, 2001.

[9] M.A. Green, K. Emery, D.L. King, S. Igari, and W. Warta. Solar cell efficiency tables (version 22). *Progress in Photovoltaics: Research and Applications*, 11:347–352, 2003.

[10] M.D. Griffin and J.R. French. *Space Vehicles Design and Construction*. AIAA Education Series, 1991.

[11] R.L. Forward and R.P. Hoyt. Failsafe multiline hoytether lifetimes. *1st AIAA/SAE/ASME/ASEE Joint Propulsion Conference, San Diego, CA, AIAA Paper 95-28903*, July 1995.

[12] T.H. Sweetster. An estimate of the golbal minimum DV needed for the earth-moon transfer. *AAS/AIAA Spaceflight Mechanics Meeting*, 1991. AAS/AIAA Paper No. 91-101.

[13] E. Mouterde, M.P. Cartmell, and Y. Wang. Computational simulation of feedback linearised control of a motorised momentum exchange tether on a circular earth orbit. *6th World Congress on Computational Mechanics, Beijing Hotel, Beijing, China*, 5-11 September 2004.

Appendix 1 - Figures

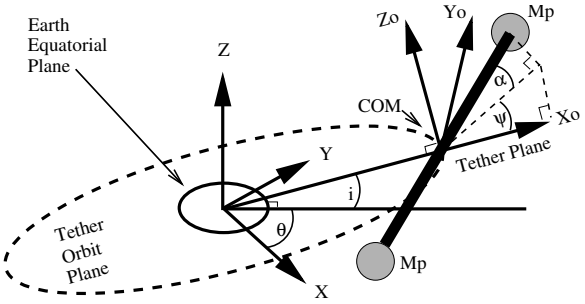

1.1: Dumb-bell Before Rotations in Tether Axis

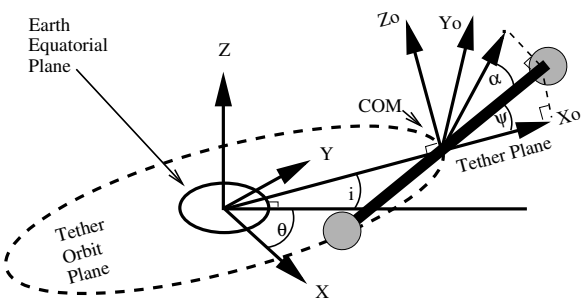

1.2: Dumb-bell After α Rotation in Tether Axis

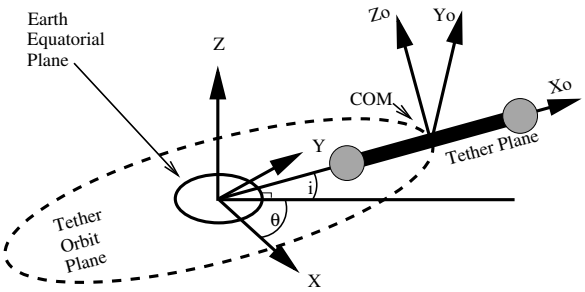

1.3: Dumb-bell After ψ Rotation in Tether Axis

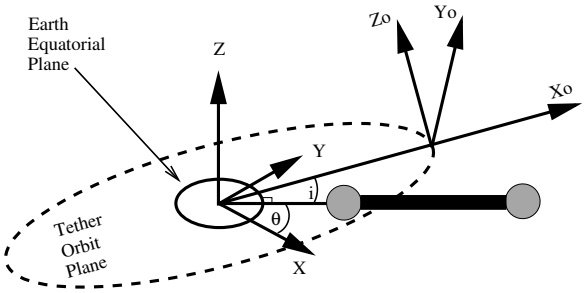

1.4: Dumb-bell After i Rotation in Inertial Axis

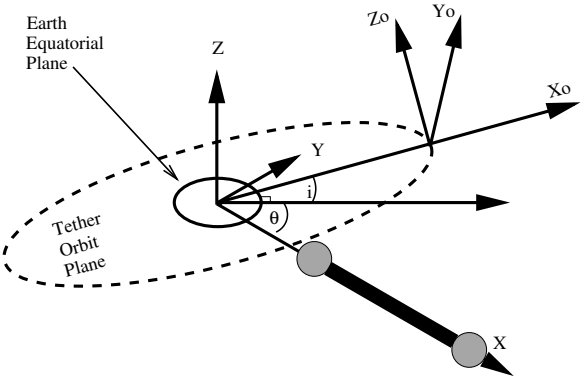

1.5: Dumb-bell After θ Rotation in Inertial Axis

Figure 1: Dumb-bell Rotations

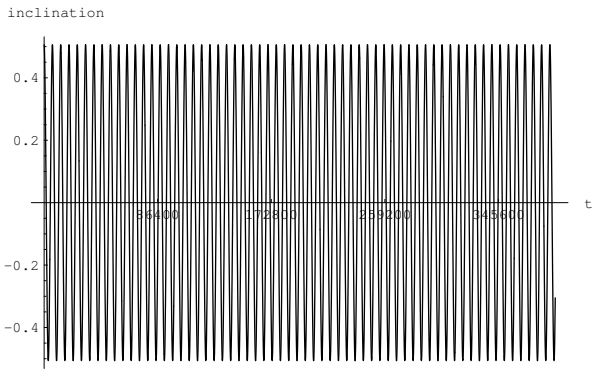

2.1: Inclination vs. Time

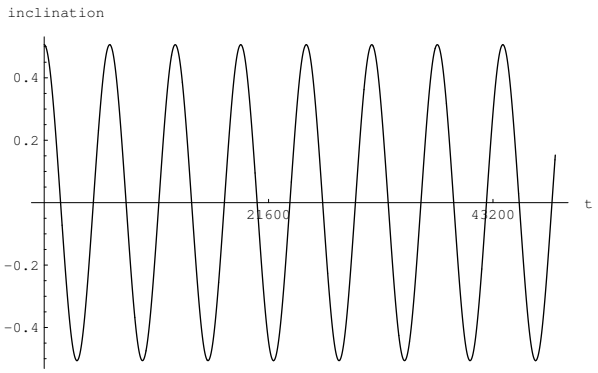

2.2: Inclination vs. Time in Detail

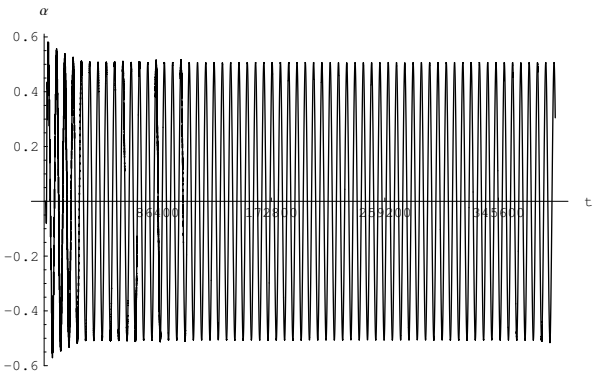

2.3: Alpha vs. Time

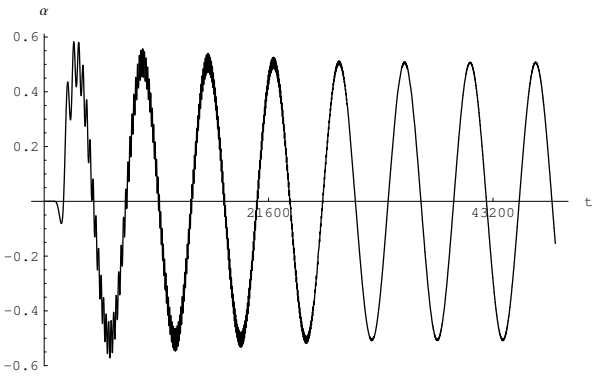

2.4: Alpha vs. Time in Detail

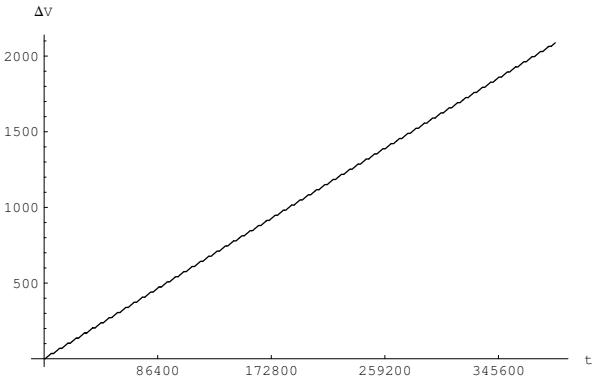

2.5: ΔV vs. Time

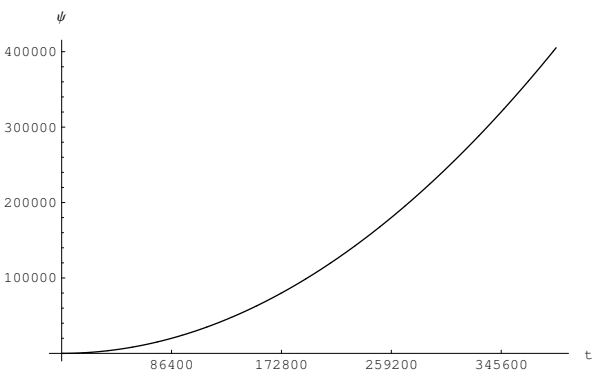

2.6: Psi vs. Time

Figure 2: Simulation Analysis

Appendix 2 - Equations of Motion

The equations of motion the MMET (stator arm not included) for the generalized co-ordinates $i, \psi, \alpha, R, \theta$ are:

$$2\mu \sin[2i+\alpha]\sin\left[\tfrac{\psi}{2}\right]^2 L_{tether}R_{facility}\left(M_{payload}\left(\frac{1}{R_{payload1}^{3/2}}-\frac{1}{R_{payload2}^{3/2}}\right)+4M_{tether}\left(\frac{1}{R_{tether1}^{3/2}}-\frac{1}{R_{tether2}^{3/2}}\right)\right)+$$
$$\cos[i]\sin[i](M_{facility}+2(M_{payload}+M_{tether}))R_{facility}^2(\theta')^2+$$
$$\tfrac{1}{4}\sin[2(i+\alpha)]L_{tether}^2(4M_{payload}+M_{tether})(\theta'+\psi')^2+$$
$$2(M_{facility}+2(M_{payload}+M_{tether}))R_{facility}i'R_{facility}{}'+$$
$$(M_{facility}+2(M_{payload}+M_{tether}))R_{facility}^2 i''+\tfrac{1}{6}L_{tether}^2(12M_{payload}(2i''+\alpha'')+M_{tether}(5i''+3\alpha''))=0$$

$$\mu\cos[i]\cos[i+\alpha]\sin[\psi]L_{tether}R_{facility}\left(M_{payload}\left(-\frac{1}{R_{payload1}^{3/2}}+\frac{1}{R_{payload2}^{3/2}}\right)+4M_{tether}\left(-\frac{1}{R_{tether1}^{3/2}}+\frac{1}{R_{tether2}^{3/2}}\right)\right)+$$
$$\tfrac{1}{6}L_{tether}^2(-3\sin[2(i+\alpha)](4M_{payload}+M_{tether})(i'+\alpha')(\theta'+\psi')+$$
$$2(6M_{payload}+M_{tether})\psi''+3\cos[i+\alpha]^2(4M_{payload}+M_{tether})(\theta''+\psi''))$$
$$=\cos[\alpha]\cos[\gamma]Force_{payload}L_{payload}(1-Eclipse)$$

$$\mu(\cos[i+\alpha]\sin[i]-\cos[i]\cos[\psi]\sin[i+\alpha])L_{tether}R_{facility}\left(M_{payload}\left(\frac{1}{R_{payload1}^{3/2}}-\frac{1}{R_{payload2}^{3/2}}\right)+4M_{tether}\left(\frac{1}{R_{tether1}^{3/2}}-\frac{1}{R_{tether2}^{3/2}}\right)\right)+$$
$$\tfrac{1}{4}\sin[2(i+\alpha)]L_{tether}^2(4M_{payload}+M_{tether})(\theta'+\psi')^2+$$
$$\tfrac{1}{6}L_{tether}^2(12M_{payload}(i''+2\alpha'')+M_{tether}(3i''+5\alpha''))$$
$$=-\sin[\gamma]Force_{payload}L_{payload}(1-Eclipse)$$

$$\mu\left(\frac{M_{facility}}{R_{facility}^2}-M_{payload}\left(\frac{-R_{angle}L_{tether}-R_{facility}}{R_{payload1}^{3/2}}+\frac{R_{angle}L_{tether}-R_{facility}}{R_{payload2}^{3/2}}\right)-2M_{tether}\left(-\frac{2R_{angle}L_{tether}+4R_{facility}}{R_{tether1}^{3/2}}+\frac{2R_{angle}L_{tether}-4R_{facility}}{R_{tether2}^{3/2}}\right)\right)-$$
$$(M_{facility}+2(M_{payload}+M_{tether}))R_{facility}((i')^2+\cos[i]^2(\theta')^2)+$$
$$(M_{facility}+2(M_{payload}+M_{tether}))R_{facility}{}''=0$$

$$-\sin[2i](M_{facility}+2(M_{payload}+M_{tether}))R_{facility}^2 i'\theta'-\tfrac{1}{2}\sin[2(i+\alpha)]L_{tether}^2(4M_{payload}+M_{tether})(i'+\alpha')(\theta'+\psi')+$$
$$2\cos[i]^2(M_{facility}+2(M_{payload}+M_{tether}))R_{facility}\theta'R_{facility}{}'+\tfrac{1}{3}L_{tether}^2(6M_{payload}+M_{tether})\theta''+$$
$$\cos[i]^2(M_{facility}+2(M_{payload}+M_{tether}))R_{facility}^2\theta''+\tfrac{1}{2}\cos[i+\alpha]^2L_{tether}^2(4M_{payload}+M_{tether})(\theta''+\psi'')=0$$

The equations use the following substitutions:

$$\begin{aligned}
R_{payload} &= L_{tether}^2-2(\cos[i]\cos[i+\alpha]\cos[\psi]+\sin[i]\sin[i+\alpha])L_{tether}R_{facility}+R_{facility}^2\\
R_{tether} &= L_{tether}^2+4(\cos[i]\cos[i+\alpha]\cos[\psi]+\sin[i]\sin[i+\alpha])L_{tether}R_{facility}+4R_{facility}^2\\
R_{angle} &= \cos[i]\cos[i+\alpha]\cos[\psi]+\sin[i]\sin[i+\alpha]
\end{aligned}$$

and $Eclipse$ is the binary function:

$$Eclipse=\begin{cases}1 & \begin{cases}R^2(1-\cos[i^2]\cos[\theta^2])\le R_{Earth}\left(1+\frac{R\cos[\theta]}{R_{Sun}}\right)\\ \text{AND}\\ \cos[i]\cos[\theta]>0\end{cases}\\ 0 & \{\quad otherwise\end{cases}$$